

# The Duffing Oscillator : A system with Cubic Nonlinearity

Sudeep Das,\* Jishnu Bhattacharyya,† and S.R.P. Mohapatra‡

*Indian Institute of Technology*

*Kanpur - 208016*

(Dated: November 15, 2002)

The steady-state frequency response of the Duffing oscillator in the non-chaotic regime is obtained both analytically as well as numerically. The associated phenomena of *jumps* and *hysteresis* are studied. The Duffing Equation is solved numerically and the behavior of the system in the phase space is investigated at different parameter values. The system is shown to exhibit period doubling bifurcations which eventually lead to chaos.

## I. INTRODUCTION

The Duffing equation characterizes the class of oscillator systems with cubic nonlinearity. It is extremely rich in its properties showing a wide variety of nonlinear phenomena. The equation arises in a large number of physical as well as biological systems and has wide applicability.

The Duffing equation is usually written in the form ,

$$\ddot{x} + 2\gamma\dot{x} + \omega_o^2 x + \epsilon x^3 = F \cos(\omega t) \quad (1)$$

where  $\gamma$  is the coefficient of damping and  $\omega_o$  the natural frequency of oscillation. The term  $F \cos(\omega t)$  characterizes a harmonic forcing of the oscillator at an angular frequency  $\omega$ . An appropriate rescaling of  $x$  and  $t$  casts the equation to the simpler form ,

$$\ddot{x} + 2\gamma\dot{x} + x + x^3 = F \cos(\omega t) \quad (2)$$

In what follows a study of some of the most interesting aspects of this equation has been made.

## II. FREQUENCY RESPONSE

The frequency response of the oscillator is studied with the assumption that the steady state response of the system is given by ,

$$x(t) = \mathcal{A}(\omega) \cos(\omega t - \theta) \quad (3)$$

On substituting Eq.(3) into the oscillator equation (2), we obtain upon equating the coefficients of the orthogonal functions  $\cos(\omega t)$  and  $\sin(\omega t)$  on either side ,

$$-\mathcal{A} [(1 - \omega^2) + \frac{3}{4}\mathcal{A}^2] \cos(\theta) + 2\gamma\mathcal{A}\omega \sin(\theta) = F \quad (4)$$

$$\mathcal{A} [(1 - \omega^2) + \frac{3}{4}\mathcal{A}^2] \sin(\theta) - 2\gamma\mathcal{A}\omega \cos(\theta) = 0 \quad (5)$$

Squaring and adding Eqns.(4)&(5), we get the frequency response equation as

$$\mathcal{A}^2 [(1 - \omega^2) + \frac{3}{4}\mathcal{A}^2]^2 + (2\gamma\mathcal{A}\omega)^2 = F^2 \quad (6)$$

The frequency response of the oscillator for various parameter values are plotted below :

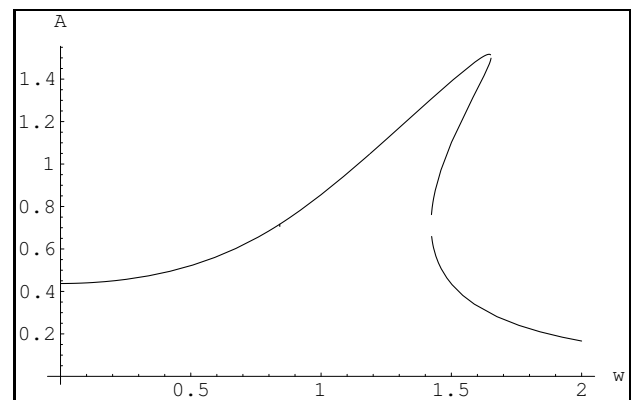


FIG. 1: Frequency response of the duffing equation with  $\gamma = 0.1$  and  $F = 0.5$ .

In the Figure 1. it is to be noted that for  $\omega$  in the range  $\sim (1.4 - 1.6)$ , the amplitude has three roots. This has important implication in the phenomenon of *hysteresis* which we shall discuss in the next section.

Figure 2. shows that as the damping is decreased, the range of  $\omega$  in which the amplitude is triple-valued increases. In Figure.3, we see that the range of  $\omega$  over which three values of  $\mathcal{A}(\omega)$  exists has decreased for increased damping. Finally when damping increases to large values, the amplitude becomes a single-valued function of  $\omega$  and hysteresis does not occur anymore (Figure.4).

When the forcing is increased, the maximum amplitude of response increases almost linearly with  $\omega_{A_{max}}$  as is seen from Figure 5.

\*Electronic address: sudeep@iitk.ac.in

†Electronic address: jishnub@iitk.ac.in

‡Electronic address: satyaray@iitk.ac.in

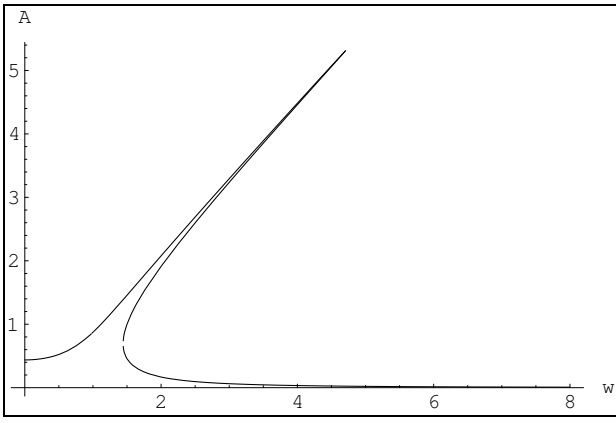


FIG. 2: Frequency response of the duffing equation with  $\gamma = 0.01$  and  $F = 0.5$ .

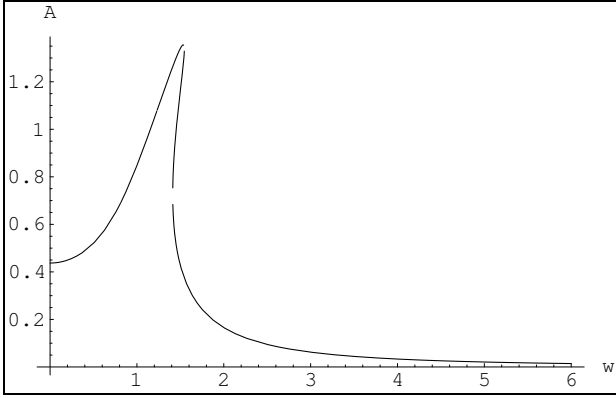


FIG. 3: Frequency response of the duffing equation with  $\gamma = 0.12$  and  $F = 0.5$ .

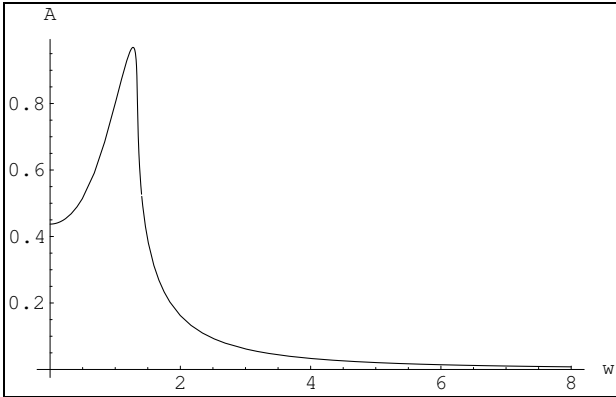


FIG. 4: Frequency response of the duffing equation with  $\gamma = 0.15$  and  $F = 0.5$ .

### III. HYSTERESIS AND JUMPS

An interesting phenomenon which occurs as a consequence of triple-valuedness of amplitude is hysteresis [1].

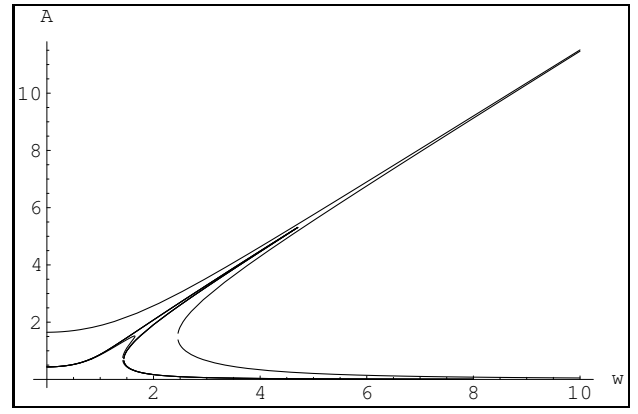


FIG. 5: Frequency response of the duffing equation with  $\gamma = 0.01$  and  $F = 0.05, F = 0.5$  and  $F = 5.0$

In Figure.6, there are three roots of  $\mathcal{A}(\omega)$  and  $\delta(\omega)$  in the interval  $1.4 \leq \omega \leq 1.7$ . As will be shown later, the roots on the curve BEC correspond to unstable saddle points whereas those on either AB or CD are stable centers. If an oscillator is started at low driving frequency  $\omega$  and  $\omega$  is gradually increased, then the steady state amplitude will rise along the stable curve AB upto the point B after which it abruptly jumps to the point C and continues along CD. On the other hand, if we start the oscillator at high  $\omega$  and decrease the driving frequency then the amplitude will rise along DCE. Beyond E, the only stable point lies along the curve FA. The corresponding behavior of the steady-state phase is shown in the adjacent figure. So there is again a jump from E to F. Since along the two directions of changing  $\omega$  the jumps occur at different points this phenomenon is called *hysteresis*.

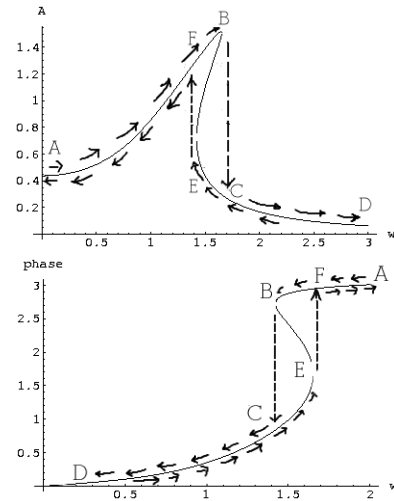


FIG. 6: The phenomena of hysteresis and jumps. The figure on top shows the steady state amplitude as a function of  $\omega$  while the figure below shows the steady-state phase as a function of  $\omega$

## A. Stability

The above discussion of hysteresis rests upon the statement that the roots on the curve BC represent unstable points whereas the roots on the curves AB and CD are stable. To show this we shall consider a solution of the Duffing Equation ( Eq.2) in the form :

$$x(t) = A(t)\cos(\omega t) + B(t)\sin(\omega t) \quad (7)$$

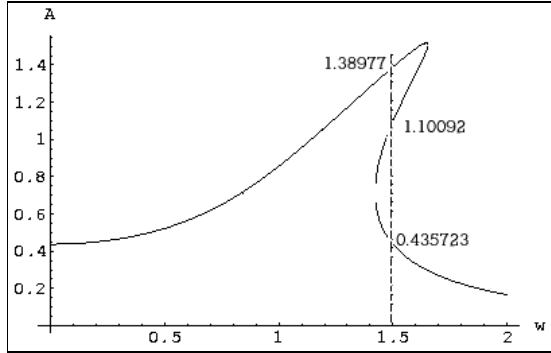
where  $A(t)$  and  $B(t)$  are time dependent amplitudes.

Substituting this into Eq.2. we obtain the differential equations for  $A(t)$  and  $B(t)$  as,

$$\begin{aligned} \ddot{A}(t) + 2\gamma\dot{A}(t) + (1 - \omega^2)A(t) + 2\omega[\dot{B}(t) + \gamma B(t)] \\ + \frac{3}{4}[A^3(t) + A(t)B^2(t)] = F \quad (8) \end{aligned}$$

$$\begin{aligned} \ddot{B}(t) + 2\gamma\dot{B}(t) + (1 - \omega^2)B(t) - 2\omega[\dot{A}(t) + \gamma A(t)] \\ + \frac{3}{4}[B^3(t) + B(t)A^2(t)] = 0 \quad (9) \end{aligned}$$

From the numerical solution of these coupled equations we can obtain a plot of the amplitude  $A = \sqrt{A^2 + B^2}$  versus the phase  $\delta = \tan^{-1}(B/A)$  with time as the parameter. From our steady-state study we should expect that a trajectory in the  $(A(t), \delta(t))$  plane would spiral into their steady-state stable points. As a specific example we study the case where  $\omega = 1.5$ ,  $F = 0.5$  and  $\gamma = 0.1$ . The steady state frequency response corresponding to these parameters are plotted in Fig.1 which we again reproduce here in Fig.7. for reference. The above figures



show the steady state roots of  $A$  and  $\delta$  for  $\omega = 1.5$ . On the  $(A(t), \delta(t))$  plane these are the points ,  $p1 = (0.435723, 2.87709)$ ,  $p2 = (1.10092, 2.42004)$  and  $p3 = (1.38977, 0.986063)$ .

Now to be in accord with our explanation of hysteresis, the point  $p2$  should be an unstable saddle point while the points  $p1$  and  $p3$  should be stable nodes. That this is actually the situation is borne out by the plot below. Here we notice that all trajectories have spiraled either into  $p1$  or  $p3$  even when the initial position is near  $p2$ .

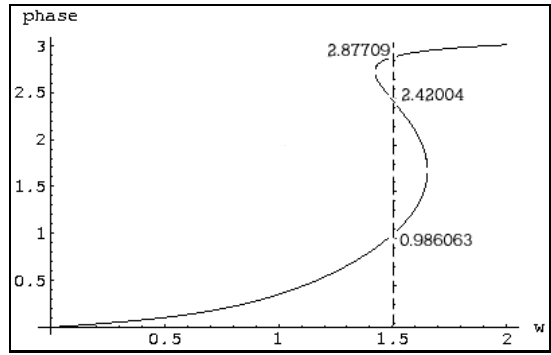


FIG. 8: The steady state roots of  $\delta$  for  $\omega = 1.5$

## IV. STUDIES IN THE PHASE PLANE

The Duffing Oscillator exhibits a wide variety of phenomena on the phase  $(x, \dot{x})$  plane. For very low forcing the phase space trajectory is an ellipse, the motion being almost simple harmonic with period equal to that of the driving force ( Fig.9).

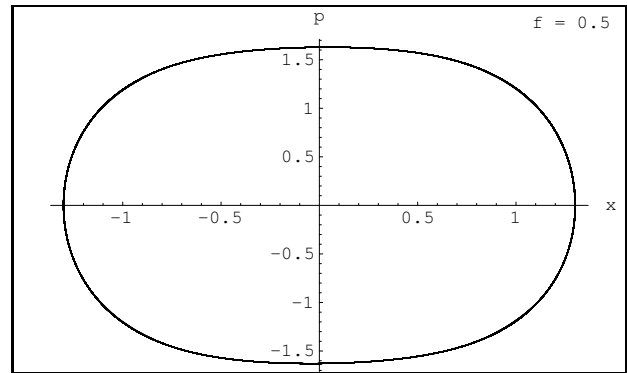


FIG. 9: The phase trajectory for  $F = 0.5$ ,  $\gamma = 0.1$ ,  $\omega = 1.4$

As the forcing is increased the effect of nonlinearity creeps in and the response no longer remains sinusoidal.

The phase-space trajectory becomes distorted.( Fig.10).

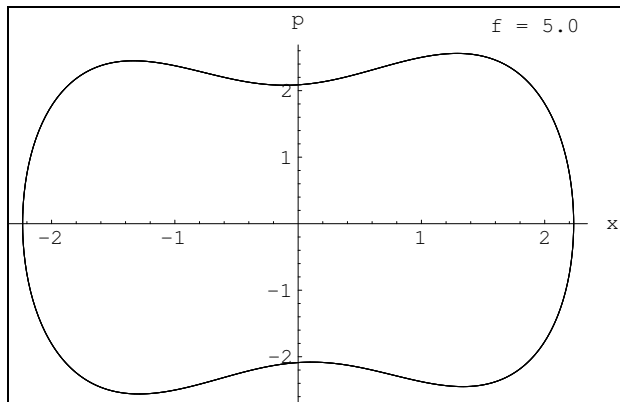


FIG. 10: The phase trajectory for  $F = 5$  ,  $\gamma = 0.1$  ,  $\omega = 1.4$

As the forcing is increased further an interesting phenomenon sets in. The oscillator does not return to initial phase point after one period of the driving force. It returns only after two such time-periods have elapsed. This is the so-called “Period-doubling”. It is convenient to look for period-bifurcations in what is called the **Poincare Section** If we take snapshots of the time-evolving phase-point at regular intervals of time ( usually the fundamental period) , then the set of points obtained is the Poincare Section. If the motion has the period same as the fundamental, then the Poincare section will be a single point. This is easy to understand because if we take snapshots of the phase point after each interval  $T$ , say, and if the point returns to its initial position with the same period  $T$  then every time we will be sampling the same point. However if we have  $n$  points on the Poincare section, then it indicates that the motion has a period  $nT$ . For  $F=20$  in the system we have been considering so far we see a period two trajectory (Fig.11).In the Poincare section we find two points as expected.

As we further increase  $F$  to 24.8 we observe a period -three response.(Fig 12).

This trend continues and we land upon a period-4 response at  $F=25.2$ .(Fig.13)

Another beautiful phenomenon on the phase plane is the occurrence of phase-trajectories which are mirror reflections of each other about both the axes. If we resolve the Duffing Equation into two first-order equations as :

$$\dot{x} = y \quad (10)$$

$$\dot{y} = -2\gamma y - x - x^3 + f \cos(\omega t) \quad (11)$$

then we shall notice that they are invariant under the substitutions  $x \rightarrow -x$  and  $y \rightarrow -y$ . and  $t \rightarrow t + \frac{\pi}{\omega}$ . Let us call this group of transformations  $\mathcal{S}$ . Hence there can be two types of orbits: orbits  $\{x(t),y(t)\}$  which are symmetric under  $\mathcal{S}$  like the ellipse in Fig(9) and orbits which are not, like the one in Fig.11. The existence of the symme-

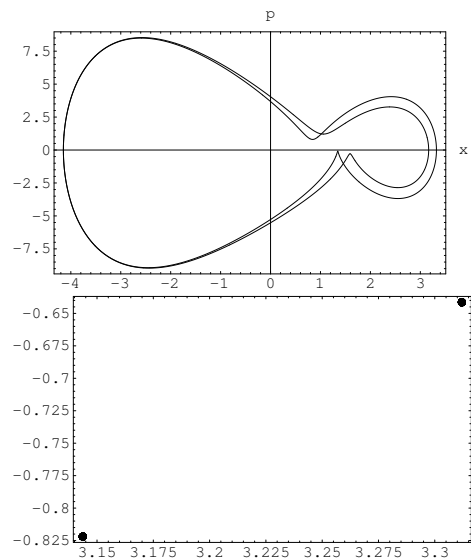


FIG. 11: The period-2 response at  $F=20$  ,  $\gamma = 0.1$  ,  $\omega = 1.4$ .The adjacent Poincare section has two points.

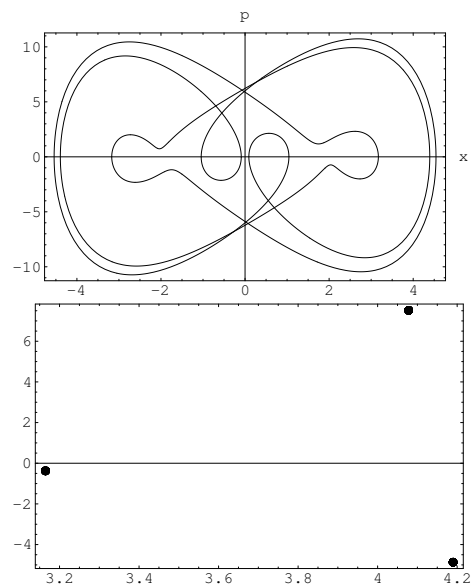


FIG. 12: The period-3 response at  $F=24.8$  ,  $\gamma = 0.1$  ,  $\omega = 1.4$ .The adjacent Poincare section has three points.

try  $\mathcal{S}$  implies that for these orbits there will exist a conjugate orbit which will look mirror-reflected about both axes. This is illustrated in Fig.14, where the change in initial conditions has resulted in reflected orbits.

There is another related event.If we slowly increase the forcing keeping the initial point fixed, the phase trajectory first evolves smoothly i.e. gets slowly modified retaining the initial shape. However, it often happens that at some value of  $F$  the trajectory switches to its reflected conjugate. This is illustrated below. This may be explained as follows.For a given forcing,there are sets

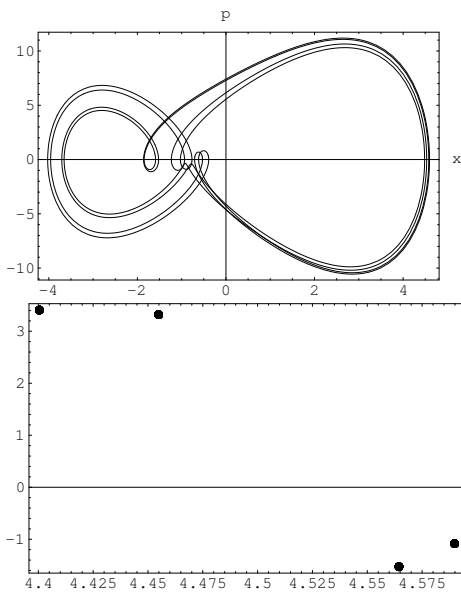


FIG. 13: The period-4 response at  $F=25.2$ ,  $\gamma = 0.1$ ,  $\omega = 1.4$ . The Poincaré section has four points.

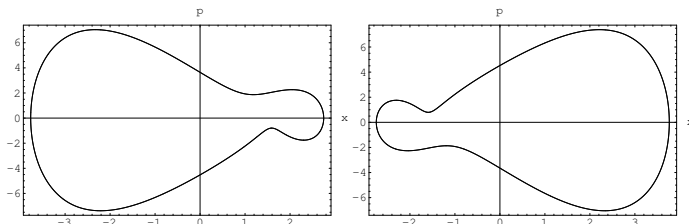


FIG. 14: The antisymmetric orbits. The left one is for initial condition  $x_o = -1$ ,  $y_o = 1$  while the right one is for the initial condition  $x_o = 1$ ,  $y_o = 1$

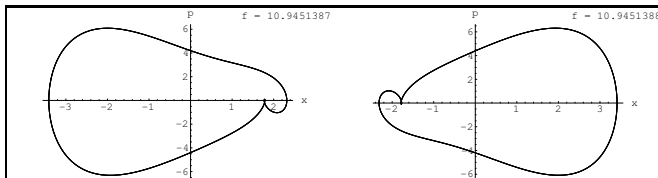


FIG. 15: The orbit switches discontinuously from one configuration to its reflected conjugate at a sharp value of forcing.

of initial conditions on the phase space which will lead to one or the other of the conjugate pairs. These initial conditions are clustered in the phase-space as non-intersecting patches. When the forcing is changed, these patches deform. It may happen that a phase point which was well within one such patch may, at a particular value of forcing come at the boundary between two such patches. Then on an infinitesimal change of forcing, the trajectory switches to the reflected counterpart.

For a certain set of parameter values, the period-doubling of the Duffing oscillator keeps on occurring for increasing value of the forcing amplitude. This eventually leads to the situation when the system has practically an infinite period. The motion therefore becomes aperiodic but remains bounded. The phase trajectories starting from any phase point ends up into a limited area of the phase space and remains forever bounded in it. This attracting set is neither an equilibrium point, nor quasiperiodic and is called a **strange attractor**[2]. It is an attractor in the sense that after the transients have died the phase-space trajectories will end up inside this geometrical structure. Inside the strange attractor, none of the trajectory is closed. The trajectories are non-intersecting and exponentially diverge away from each other. Due to this later property, the system exhibits extreme sensitivity to initial conditions and the motion is completely unpredictable. This means that the system has turned chaotic. Another interesting aspect is that although within the attractor the non-intersecting trajectories diverge exponentially from each other, they do not fill the whole phase space. The strange attractor is thus a fractal having a dimension between one and two. In the Poincaré section the strange attractor appears as a set of infinite points inside a structure having a definite shape. This shape is practically independent of initial conditions. The strange attractor in the Poincaré section is shown in Fig.17. The fact that the strange attractor

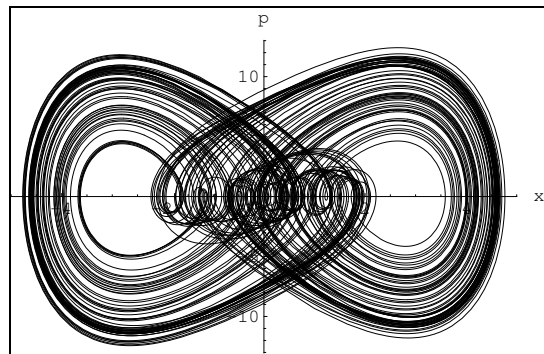


FIG. 16: The chaotic phase trajectory for  $F = 25$ ,  $\gamma = 0.1$ ,  $\omega = 1.3$

has a definite shape irrespective of the fact that the trajectories inside it are diverging shows that the system though apparently chaotic has some kind of order in it.

## V. POWER SPECTRUM ANALYSIS

A powerful tool for investigating dominant frequencies in the response of a nonlinear oscillator is the **Fourier Transform**.

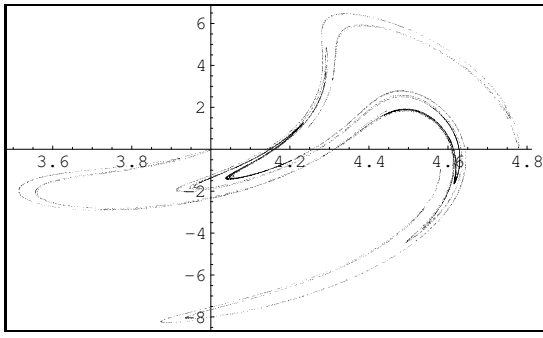


FIG. 17: The strange attractor on the Poincare section

From the numerical solution of the Duffing Equation (Eq.1), we have sampled  $N$  values of the co-ordinate  $x(t)$  at equally spaced points in time. On the data set  $(x_0, x_1, x_2, \dots, x_N)$  so obtained, we have performed a **discrete Fourier Transform**

$$f_k = \frac{1}{\sqrt{N}} \sum_{j=0}^N x_j e^{-\frac{2\pi i k j}{N}}, \quad (k = 0, 1, 2, \dots, N-1) \quad (12)$$

What the Fourier Transform basically does is to single out the various frequency components present in the signal. Here  $f_k$ , which is in general complex, provides a measure of the weight with which the frequency  $\omega_k$  contributes to the signal. We define the **power spectrum**[3] by :

$$P(\omega_k) = f_k \bar{f}_k = |f_k|^2$$

A sharp peak in the  $P(\omega_k)$  versus  $\omega_k$  plot will indicate that the particular frequency is dominant.

As a simple illustration, let us consider the case when the forcing is low and the response is period-1 with the frequency of the driving force. Here we should expect a power spectrum with a single peak at the forcing frequency. Fig.18 shows that this is indeed the case.

Fig.19 shows the power-spectrum of for a period-2 response. Here we should expect a peak at the driving frequency  $\omega$  and another peak at  $\frac{\omega}{2}$  which we indeed observe. However we get something extra here. There is a strong peak at  $2\omega$  indicating the strong existence of a **superharmonic**. We may note that the existence of this superharmonic is not obvious from phase plot study. This illustrates the power of the Fourier method.

However the richness of the frequency spectrum is observable in the case when the oscillator enters the chaotic regime. The power spectrum in this case is shown in Fig.20.

This power-spectrum shows that the oscillator though driven by a single frequency has dominant responses at a large number of different frequencies. Extremely prominent among them is the **superharmonic** at  $3\omega$  and the **subharmonics** of frequency  $\frac{\omega}{6}$  and  $\frac{\omega}{3}$ . These show that the Duffing Oscillator has considerable response at frequencies which are integral multiples and sub-multiples

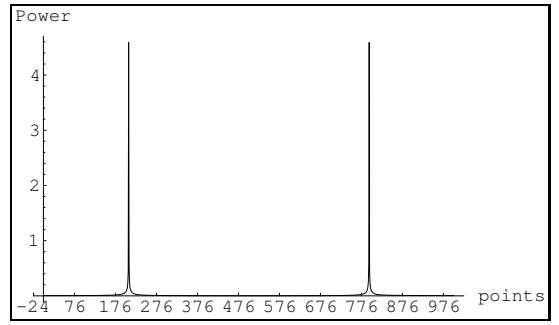


FIG. 18: The power-spectrum for  $F = 0.2$ ,  $\gamma = 0.1$ ,  $\omega = 1.4$ . This plot generated in *Mathematica* is interpreted as follows. We observe a peak at 223 and a symmetric peak at  $(1000 - 223) = 777$ . This basically means that there is a single dominant frequency component with frequency  $223/1000 = 0.223$ . This frequency is exactly the driving frequency  $\frac{\omega}{2\pi} = 0.223$ .

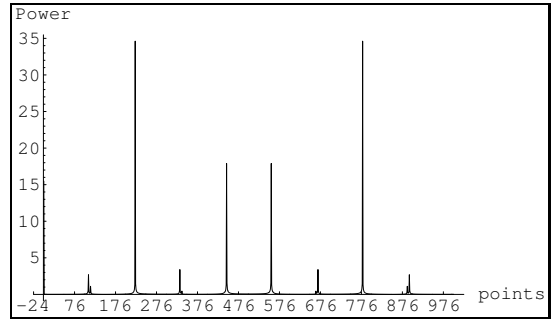


FIG. 19: The power-spectrum for  $F = 10$ ,  $\gamma = 0.1$ ,  $\omega = 1.4$ . This plot generated in *Mathematica* is interpreted as follows. We observe a peak at 223 and a symmetric peak at  $(1000 - 223) = 777$ . This corresponds to a frequency component with frequency  $223/1000 = 0.223$ . This frequency is exactly the driving frequency  $\nu_0 = \frac{\omega}{2\pi} = 0.223$ . We also note a peak at 111.5, corresponding to the frequency  $111.5/1000 = 0.1115$  corresponding to  $\frac{\nu_0}{2}$ . There is also a strong peak at 446, which corresponds to the frequency  $2\nu_0$ .

of the driving frequency. This points to the possibility that the oscillator will exhibit large amplitude responses at these frequencies. In fact such response are observed in experiments and are called subharmonic and superharmonic resonances.

## VI. CONCLUSION

In this report we have made quite a detailed study of the Duffing Oscillator system. We have investigated a rich spectrum of phenomena which delineates the importance of the Duffing Equation as a model of nonlinear systems.

1. We have observed and analyzed the phenomena of Jumps and Hysteresis.

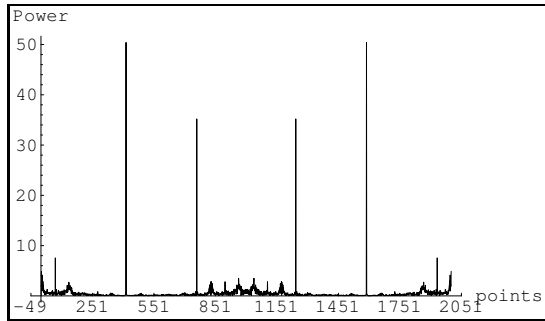


FIG. 20: The power-spectrum for  $F = 25$ ,  $\gamma = 0.1$ ,  $\omega = 1.3$ . This *Mathematica* plot is interpreted as follows. The full horizontal scale here is 2000. We observe the mightiest peak at 414 (and its companion peak at  $2000 - 414$ ). Thus the frequency is  $414/2000 = 0.207$ . This is the response at the driving frequency  $\frac{\omega}{2\pi} = \nu_0$ . The next dominant frequency is at 1242 (with symmetric companion at  $2000 - 1242 = 758$ ) which corresponds to  $3\nu_0$ . Other prominent peaks are at 138 corresponding to  $\frac{\nu_0}{3}$ , at 69 corresponding to  $\frac{\nu_0}{6}$ .

2. We have analyzed the stability behavior of the system in order to explain these phenomena.
3. The study has then been extended to the phase-space behavior of the system where we have shown the effects of nonlinearity in the form of deviation

from simple harmonic behavior.

4. Another signature of nonlinearity is the occurrence of period- $n$  bifurcations which we have studied in quite detail.
5. In this connection we have generated the Poincare sections, which by far remains one of the most powerful tools for probing chaotic systems.
6. We have followed the system to chaos through period doubling bifurcations. The strange attractor has been obtained and its strange properties have been discussed.
7. We have extended the study to the investigation of subharmonic and superharmonic responses of the oscillator. This may be done analytically by perturbation methods. We have resorted to the numerical strategy by obtaining a Fourier transform of the timeseries response. The peaks in this power spectrum of the chaotic oscillator has indicated the existence of harmonics other than the fundamental.

Scope remains of extending this study into the challenging inquiry of calculating the Lyapunov Exponent for this system and to study the bifurcations in more detail to determine whether the system gives the universal Feigenbaum number.

- 
- [1] **Nayfeh, A.H & Mook, D.T**, *Nonlinear Oscillations*, John Wiley & Sons, New York, 1979.
  - [2] **Gukenheimer, J & Holmes, P**, *Nonlinear Oscillations, Dynamical Systems & Bifurcation of Vector Fields*,

Springer Verlag, 1983.

- [3] **D.W. Jordan, P. Smith**, *Nonlinear Ordinary Differential Equations*, 2nd edition, OUP, 1987.